Revista Eletrônica
Paulista de Matemática

ISSN 2316-9664
v. 22, n. 2, set. 2022
Edição Brazilian Symposium on
Fractional Calculus

Numerical study of the parameters in an arbitrary order SIR model built with Mittag-Leffler distribution

Noemi Zeraick Monteiro
Universidade Federal de Juiz de Fora
nzmonteiro@ice.ufjf.br

Sandro Rodrigues Mazorche
Universidade Federal de Juiz de Fora
sandro.mazorche@ufjf.edu.br

Abstract

We previously discussed the construction of an arbitrary order SIR model with physical meaning. We believe that arbitrary order derivatives can be obtained through Mittag-Leffler based laws in the infectivity and removal functions. Here we are interested in obtaining information about the influence of the parameters in the studied model, with the aim of promoting its use and strengthening the biological interpretation.

Keywords: Arbitrary order derivatives. SIR model. Mittag-Leffler. Parameter analysis.

1 Introduction

The most used operators in the Arbitrary Order Calculus, more known as Fractional Calculus, are non local, which allows consider the dependence of previous stages. Therefore, many times, the substitution of the integer orders in an ODE system by non integer ones is called the considering of "memory effect".

Throughout our research, we publish some works about the meaning difficulty, loss of properties and the lack of the construction of fractional SIR type models ((MAZORCHE; MONTEIRO, 2021), (MONTEIRO; MAZORCHE, 2021e), (MONTEIRO; MAZORCHE, 2021f)). In this context, we study a model by Angstmann, Henry and McGann (ANGSTMANN; HENRY; MCGANN, 2017) in which the arbitrary order derivatives are obtained by construction, considering Mittag-Leffler functions and generalizing the infectivity and remotion functions. We seek to extend some results in the discussion of the model in (MONTEIRO; MAZORCHE, 2021a), (MONTEIRO; MAZORCHE, 2021b) and, as started in (MONTEIRO; MAZORCHE, 2021c), (MONTEIRO; MAZORCHE, 2021e), we have been working in applications of the model to COVID-19.

The propose of the present work is, after some preliminary presentations, to expand the numerical results started in (MONTEIRO; MAZORCHE, 2021d). We revisited the authors' work and built an L1-scheme based discretization to the model, discussing numerical features at Section 4. The outcome is a more deep knowledge of the parameters and orders' effect, what is an important supporting in the mathematical and epidemiological understanding of the model. This is pretty relevant, once the model is still almost totally unexplored.

2 The Fractional Calculus

In this Section, we present the main definitions and results used in the work. The Fractional Calculus has been shown to be a very useful tool in capturing the dynamics of the physical process of several scientific objects, being generally related to the "memory effect". Probably, it was born in 1695, when l'Hôpital asked Leibniz about the meaning of a derivative of order $1/2$. Over the next centuries, important advances were made by Liouville, Riemann, Grünwald, Caputo, and many others. However, it was only after the first International Conference on Fractional Calculus and Applications, in 1974, that the number of researchers in Fractional Calculus showed great growth. Currently, congresses and symposia take place more frequently, and the reader may refer to the reference (OLIVEIRA, 2019) for a chronology of publications in Fractional Calculus until 2019, as well as for general results.

Below we consider $[a, b]$ a finite real interval, and α a real number such that $0 \leq n-1 < \alpha < n$, with n integer. The extension of the idea of the iterated integral leads to the following definition:
Definition 1: Riemann-Liouville integral in finite intervals. The Riemann-Liouville integral of an arbitrary order α is set to $t \in [a, b]$ by

$$I^{\alpha}_{a+} f(t) = \frac{1}{\Gamma(\alpha)} \int_a^t (t-\theta)^{\alpha-1} f(\theta) d\theta. \tag{1}$$

After introducing the arbitrary order integral, it is natural to search for the definition of the correspondent derivative:
Definition 2: Riemann-Liouville derivative in finite intervals. The Riemann-Liouville derivative of an arbitrary order α is set to $t \in [a, b]$ by

$$D^{\alpha}_{a+} f(t) = D^n [I^{n-\alpha}_{a+} f(t)] = \frac{1}{\Gamma(n-\alpha)} \left(\frac{d^n}{dt^n}\right) \int_a^t (t-\theta)^{n-\alpha-1} f(\theta) d\theta\,, \tag{2}$$

with D^n representing the integer-order derivative.

Finally, we present the Mittag-Leffler functions with one, two, and three parameters. The classic Mittag-Leffler function, due to its importance in several arbitrary order differential equations, was nicknamed the "queen of special functions" of the Fractional Calculus. Its importance for Fractional Calculus resembles the importance of the exponential function for classical calculus. We present the following definition (OLIVEIRA, 2019):

Definition 3: Mittag-Leffler function with one, two, and three parameters. Let z be a complex number, and three parameters α, β complex, and ρ real, such that $Re(\alpha) > 0, Re(\beta) > 0, \rho > 0$. We define the Mittag-Leffler function with three parameters through the power series

$$E^{\rho}_{\alpha,\beta}(z) = \sum_{k=0}^{\infty} \frac{(\rho)_k}{\Gamma(\alpha k + \beta)} \frac{z^k}{k!}, \tag{3}$$

where $(\rho)_k$ is the Pochhammer symbol, defined by $(\rho)_k = \Gamma(\rho + k)/\Gamma(\rho)$.

Particularly, when $\rho = 1$, we have $(\rho)_k = k!$, and the two-parameter Mittag–Leffler function, denoted simply by $E^1_{\alpha,\beta}(t) = E_{\alpha,\beta}(t)$. When $\rho = \beta = 1$, we obtain the classic Mittag-Leffler function, denoted by $E^1_{\alpha,1}(t) = E_{\alpha,1}(t) = E_{\alpha}(t)$. We point out that this function generalizes the exponential function, being equal to it when $\alpha = \beta = \rho = 1$.

3 The model

We present in (MONTEIRO; MAZORCHE, 2021e) a physical derivation following the steps of Angstmann, Henry & McGann (ANGSTMANN; HENRY; MCGANN, 2017), which use the probabilistic language of Continuous Time Random Walks (PATC), and Mittag-Leffler functions. The following is a brief note about the construction of the model.

Consider an individual infected since the time t'. If there are $S(t)$ susceptible in time t, this infected person has a probability $S(t)/N$ that his contact is susceptible, considering the population homogeneous. Therefore, in the period of t to $t + \Delta T$, the expected number of new infections per infected individual is given by $\sigma(t, t')S(t)\Delta T/N$. The transmission rate per infectious individual $\sigma(t, t')$ depends on both the age of the infection, $t - t'$, and the present time, t. The probability that an individual infected at the moment t' is still infected at the moment t is given by the survival function $\Phi(t, t')$. Therefore, the flux of individuals to the I compartment in a time t is recursively given by

$$q^+(I, t) = \int_{-\infty}^{t} \sigma(t, t') \frac{S(t)}{N} \Phi(t, t') q^+(I, t') dt'. \tag{4}$$

The initial condition is obtained by the number of individuals infected at the time 0, and considering the time in which each individual has become infected. This is given by the function $i(-t', 0)$ which represents the number of individuals who are still infectious at time 0 and who were originally infected at some point earlier $t' < 0$. Then $q^+(I, t') = i(-t', 0)/\Phi(0, t')$ for $t' < 0$. For simplicity, we consider $i(-t, 0) = i_0\delta(-t)$, where $\delta(t)$ is the Dirac delta function. So,

$$q^+(I, t) = \int_{0}^{t} \sigma(t, t') \frac{S(t)}{N} \Phi(t, t') q^+(I, t') dt' + i_0 \sigma(t, 0) \frac{S(t)}{N} \Phi(t, 0). \tag{5}$$

The historic is considered completely, avoiding doubts about the starting point. However, the model is singular at the 0. The infection rate $\sigma(t, t')$ is assumed to be a function of both the current time (due, for example, to containment measures), having an extrinsic infectivity ω, and the age of infection $t - t'$, having an intrinsic infectivity ρ. So, we can write

$$\sigma(t, t') = \omega(t)\rho(t - t'). \tag{6}$$

Assuming that the natural death and the removal of an infected individual are independent processes, we can write the survival function as

$$\Phi(t,t') = \phi(t-t')\theta(t,t'), \tag{7}$$

where $\phi(t-t')$ is the probability that an individual infected since t' has not yet recovered or been killed by the disease at time t. Also, $\theta(t,t')$ is the probability that an infected individual since t' has not yet died of natural death (that is, independent of the disease) until time t. The θ function is given by $\theta(t,t') = e^{-\int_{t'}^{t}\gamma(u)du}$, where γ is the death rate.

Individuals in the I compartment at time t must have entered this compartment at some time before and remained in it until t. Therefore, we can express the number of infected individuals as

$$I(t) = I_0(t) + \int_0^t \Phi(t,t')q^+(I,t')dt', \tag{8}$$

where the $I_0(t)$ function provides the number of individuals who were infected at 0 and remain infectious at t. With this information, we can build the principal equations of the model. We start by deriving Eq. 8 through the Leibniz Rule, obtaining

$$\frac{dI(t)}{dt} = q^+(I,t') - \int_0^t \psi(t-t')\theta(t,t')q^+(I,t')dt' - \gamma(t)\int_0^t \phi(t-t')\theta(t,t')q^+(I,t')dt' + \frac{dI_0(t)}{dt}, \tag{9}$$

where $\psi(t) = -d\phi(t)/dt$. This ψ has an important relationship with the continuous random variable X that provides the time of removal of the individual from the infectious compartment. The cumulative distribution of X, namely F defined by $F(t) = P(X \leq t)$, is such that $F(t) = 1 - \phi(t)$. Therefore, the probability density function of X is $\psi(t) = -d\phi(t)/dt$.

In what follows, we define infectivity and recovery memory kernels

$$K_I(t) = \mathcal{L}^{-1}\left\{\frac{\mathcal{L}\{\rho(t)\phi(t)\}}{\mathcal{L}\{\phi(t)\}}\right\} \quad , \quad K_R(t) = \mathcal{L}^{-1}\left\{\frac{\mathcal{L}\{\psi(t)\}}{\mathcal{L}\{\phi(t)\}}\right\}, \tag{10}$$

so we can state the set of equations for the SIR model in a similar manner to that written originally by Kermack and McKendrick (KERMACK; MCKENDRICK, 1991):

$$\frac{dS(t)}{dt} = \gamma(t)N - \omega(t)\frac{S(t)}{N}\theta(t,0)\int_0^t K_I(t-t')\frac{I(t')}{\theta(t',0)}dt' - \gamma(t)S(t), \tag{11}$$

$$\frac{dI(t)}{dt} = \omega(t)\frac{S(t)}{N}\theta(t,0)\int_0^t K_I(t-t')\frac{I(t')}{\theta(t',0)}dt' - \theta(t,0)\int_0^t K_R(t-t')\frac{I(t')}{\theta(t',0)}dt' - \gamma(t)I(t), \tag{12}$$

$$\frac{dR(t)}{dt} = \theta(t,0)\int_0^t K_R(t-t')\frac{I(t')}{\theta(t',0)}dt' - \gamma(t)R(t), \tag{13}$$

where we consider the same rate $\gamma(t)$ of natural mortality in each compartment, with the birth rate equal to that. In this case the population remains constant.

We choose $\psi(t)$ with potential law and $\rho(t)$ related to the choice of $\psi(t)$. In particular, we use the Mittag-Leffler function, according to Definition 3, in order to generalize the exponential distribution of the random variable X, which, as said, provides the removal time of the individual from the infectious compartment. As we shall see, this choice is related to the emergence of arbitrary order derivatives in the model. So, we do

$$\psi(t) = \frac{t^{\alpha-1}}{\tau^\alpha}E_{\alpha,\alpha}\left(-\left(\frac{t}{\tau}\right)^\alpha\right), \tag{14}$$

for $0 < \alpha \leq 1$, where τ is a scale parameter. Thus, the correspondent survival function is

$$\phi(t) = E_{\alpha,1}\left(-\left(\frac{t}{\tau}\right)^{\alpha}\right). \tag{15}$$

We can calculate the Laplace transform of the recovery memory kernel with Mittag-Leffler distribution, obtaining

$$\mathcal{L}\{K_R(t)\} = \frac{\mathcal{L}\{\psi(t)\}}{\mathcal{L}\{\phi(t)\}} = s^{1-\alpha}\tau^{-\alpha}. \tag{16}$$

On the other hand, we have $\mathcal{L}\{D^{1-\alpha}_{0+}f(t)\} = s^{1-\alpha}\mathcal{L}\{f(t)\} - I^{\alpha}_{0+}f(t)\mid_{t=0^+}$. We consider here $I^{\alpha}_{0+}f(t)\mid_{t=0^+}= 0$, as in (ANGSTMANN; HENRY; MCGANN, 2017). Hereafter, for simplicity, we write $D^{1-\alpha}$ in place of $D^{1-\alpha}_{0+}$. From these considerations, a convolution with the recovery memory kernel can be written as

$$\int_0^t K_R(t-t')\frac{I(t')}{\theta(t',0)}dt' = \tau^{-\alpha}D^{1-\alpha}\left(\frac{I(t)}{\theta(t,0)}\right). \tag{17}$$

A fractional derivative can also be incorporated into the infectivity memory kernel, by considering

$$\rho(t) = \frac{1}{\phi(t)}\frac{t^{\beta-1}}{\tau^{\beta}}E_{\alpha,\beta}\left(-\left(\frac{t}{\tau}\right)^{\alpha}\right). \tag{18}$$

As $\rho(t) \geq 0$ is required, we consider $0 < \alpha \leq \beta \leq 1$. Using Eq. 18, we obtain the Laplace transform of the infectivity kernel, following that

$$\int_0^t K_I(t-t')\frac{I(t')}{\theta(t',0)}dt' = \tau^{-\beta}D^{1-\beta}\left(\frac{I(t)}{\theta(t,0)}\right). \tag{19}$$

Replacing Eq. 17 and 19 in the model 11 - 13, we obtain a meaningful arbitrary order SIR model:

$$\frac{dS(t)}{dt} = \gamma(t)N - \frac{\omega(t)S(t)\theta(t,0)}{N\tau^{\beta}}D^{1-\beta}\left(\frac{I(t)}{\theta(t,0)}\right) - \gamma(t)S(t), \tag{20}$$

$$\frac{dI(t)}{dt} = \frac{\omega(t)S(t)\theta(t,0)}{N\tau^{\beta}}D^{1-\beta}\left(\frac{I(t)}{\theta(t,0)}\right) - \frac{\theta(t,0)}{\tau^{\alpha}}D^{1-\alpha}\left(\frac{I(t)}{\theta(t,0)}\right) - \gamma(t)I(t), \tag{21}$$

$$\frac{dR(t)}{dt} = \frac{\theta(t,0)}{\tau^{\alpha}}D^{1-\alpha}\left(\frac{I(t)}{\theta(t,0)}\right) - \gamma(t)R(t). \tag{22}$$

Notice that, if $\alpha = \beta = 1$, and $\gamma(t) \equiv \gamma, \omega(t) \equiv \omega$ are considered constant, we get the simple integer-order SIR model. Finally, we remember that the probability distribution $F(t) = 1 - \phi(t)$ is a Mittag-Leffler distribution $F(t;\alpha,\tau) = 1 - E_{\alpha}\left(-(t/\tau)^{\alpha}\right)$. If $\alpha = \beta = 1$, we have an exponential distribution and the expectation (first moment) of the random variable X exists, with τ being exactly the average recovery time. When $\alpha < 1$, we do not have finite expectation.

3.1 Equilibrium

In (MONTEIRO; MAZORCHE, 2021a), we state the following results about equilibrium points.
Theorem 1. If $\omega(t)$ is limited with $\lim_{t\to\infty}\omega(t) = \omega^*$, $\gamma(t) \equiv \gamma$, and $\beta = 1$ in the system 20-22, then the disease-free equilibrium given by

$$S^* = N, \quad I^* = 0, \quad R^* = 0, \tag{23}$$

is globally asymptotically stable if $\omega^* < (\tau\gamma)^{1-\alpha} + (\tau\gamma)$.

Theorem 2. If $\gamma(t) \equiv \gamma, \omega(t) \equiv \omega$ are taken constant, and $\beta = 1$ in the system 20-22, then the endemic state given by

$$S^* = \frac{((\tau\gamma)^{\beta-\alpha} + (\tau\gamma)^{\beta})N}{\omega^*}, I^* = \frac{N(\tau\gamma)^{\alpha}}{1+(\tau\gamma)^{\alpha}} - \frac{N(\tau\gamma)^{\beta}}{\omega^*}, R^* = \frac{N}{1+(\tau\gamma)^{\alpha}} - \frac{N(\tau\gamma)^{\beta-\alpha}}{\omega^*}. \tag{24}$$

is locally asymptotically stable whenever feasible, ie, when $\omega^* > (\tau\gamma)^{1-\alpha} + (\tau\gamma)$.

Although the proofs need, for now, these restrictions, such as $\beta = 1$, the numerical results seem to show that, if $i_0 > 0$, the endemic equilibrium of Eq. 24 is globally asymptotically stable whenever feasible, this is, if $\omega^* > (\tau\gamma)^{1-\alpha} + (\tau\gamma)$, being the disease-free equilibrium globally asymptotically stable otherwise.

4 The effect of the orders and parameters

There are several numerical methods that can be applied to arbitrary order derivatives. For now, we build a numerical scheme like $L1$ (OLDHAM; SPANIER, 1974) to discretize the model described in the last Section.

4.1 Numerical scheme

The time interval $[a, t]$ is discretized as $a = t_0 < t_1 < \cdots < t_n = t$, where the time steps $\Delta T_i = t_{i+1} - t_i$, for $i \in \{0, \cdots, n-1\}$, have the same size ΔT. Considering $\alpha \in (0, 1]$, we perform the following discretization for the Riemann-Liouville derivative:

$$D_{a+}^{1-\alpha} f(t_j) \simeq \frac{\Delta T^{\alpha-1}}{\Gamma(\alpha+1)} \left[\sum_{k=0}^{j-1} f(t_k)[(j-k+1)^{\alpha} - 2(j-k)^{\alpha} + (j-k-1)^{\alpha}] + f(t_j) \right], \tag{25}$$

where $t_i = i\Delta T + t_0$ for all $i \in \{0, 1, \cdots, n\}$.

We define the following matrix expressions:

$$AI_j = [D \bullet [I(0), I(1), \cdots, I(k), \cdots, I(j-1)]] \cdot \left[\begin{bmatrix} j+1 \\ j \\ \vdots \\ j-k+1 \\ \vdots \\ 2 \end{bmatrix}^{\alpha} - 2 \begin{bmatrix} j \\ j-1 \\ \vdots \\ j-k \\ \vdots \\ 1 \end{bmatrix}^{\alpha} + \begin{bmatrix} j-1 \\ j-2 \\ \vdots \\ j-k-1 \\ \vdots \\ 0 \end{bmatrix}^{\alpha} \right], \tag{26}$$

$$BI_j = [D \bullet [I(0), I(1), \cdots, I(k), \cdots, I(j-1)]] \cdot \left[\begin{bmatrix} j+1 \\ j \\ \vdots \\ j-k+1 \\ \vdots \\ 2 \end{bmatrix}^{\beta} - 2 \begin{bmatrix} j \\ j-1 \\ \vdots \\ j-k \\ \vdots \\ 1 \end{bmatrix}^{\beta} + \begin{bmatrix} j-1 \\ j-2 \\ \vdots \\ j-k-1 \\ \vdots \\ 0 \end{bmatrix}^{\beta} \right], \tag{27}$$

$$D = \theta(j,0) \left[\frac{1}{\theta(0,0)}, \frac{1}{\theta(1,0)}, \cdots, \frac{1}{\theta(k,0)}, \cdots, \frac{1}{\theta(j-1,0)} \right] = [\theta(j,0), \theta(j-1,0), \cdots, \theta(1,0)], \tag{28}$$

with $\bullet$ representing the product coordinate to coordinate.

We finally write:

$$S(j+1) = S(j) + \Delta T\gamma(j)N - \frac{\omega(j)S(j)\Delta T^{\beta}}{N\tau^{\beta}\Gamma(\beta+1)}[BI_j + I(j)] - \Delta T\gamma(j)S(j), \tag{29}$$

$$I(j+1) = I(j) + \frac{\omega(j)S(j)\Delta T^{\beta}}{N\tau^{\beta}\Gamma(\beta+1)}[BI_j + I(j)] - \frac{\Delta T^{\alpha}}{\tau^{\alpha}\Gamma(\alpha+1)}[AI_j + I(j)] - \Delta T\gamma(j)I(j), \quad (30)$$

$$R(j+1) = R(j) + \frac{\Delta T^{\alpha}}{\tau^{\alpha}\Gamma(\alpha+1)}[AI_j + I(j)] - \Delta T\gamma(j)R(j). \quad (31)$$

That multistep scheme is used in the next Section. It is important to reiterate that the integer order case is obtained by taking $\alpha = \beta = 1$.

4.2 Parameter analysis

Now, we produce a parameter analysis in the model given in 20-22, with initial conditions $N = 1000000$, $I(0) = 1$, $S(0) = N - 1$, and $R(0) = 0$. As in most applications, we consider $\gamma(t) \equiv \gamma$, and, therefore, $\theta(t,0) = e^{-\gamma t}$. Initially, we consider $\omega(t) \equiv \omega$. Then, we study $\omega(t)$ with exponential and oscillatory decay. We also analyze the influence of the orders α, β, and the parameter τ in the functions of permanence in the infectious compartment (independent of vital dynamics), and in the intrinsic infectivity function, respectively given by

$$\phi(t) = E_{\alpha,1}\left(-\left(\frac{t}{\tau}\right)^{\alpha}\right) \quad ; \quad \rho(t) = \frac{1}{\phi(t)}\frac{t^{\beta-1}}{\tau^{\beta}}E_{\alpha,\beta}\left(-\left(\frac{t}{\tau}\right)^{\alpha}\right). \quad (32)$$

The time step used is $dt = 0.1$. We observe that, for $\beta < 1$, we have $\lim_{t\to 0+}\rho(t) = \infty$. Thus, we start the calculation of ρ at $t = 0.5$.

• (Effect of α in the functions ϕ and ρ) Figure 1 shows us that the smaller α, the heavier the tail of the permanence function ϕ in the infectious compartment. Furthermore, from Figure 2, the larger α, the smaller the intrinsic infectivity function over time.

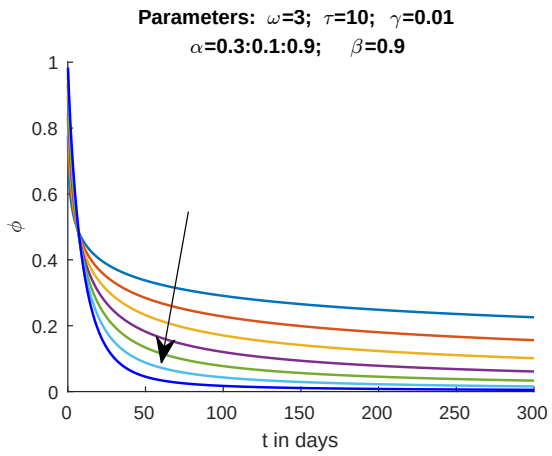

Figure 1: Effect of α in ϕ.

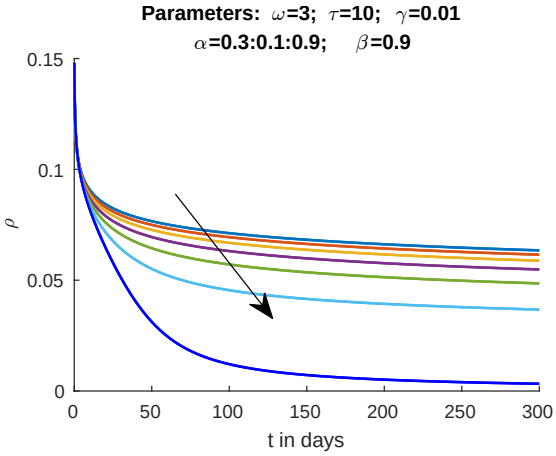

Figure 2: Effect of α in ρ.

• (Effect of α in the compartments) In Figures 3-5, we observe that the higher the α, the smaller and earlier the infection peak occurs. The amount of susceptible is re-established sooner as α grows and the wave of removed occurs in a shorter time. Decreasing the α increases the asymmetry in the distribution of infectious, reflecting the effect of α in the ϕ function, and increases the peak, reflecting the effect of α in ρ.

• (Effect of α in the equilibrium) Figure 6 illustrates the equilibrium given in Eq. 24 for different orders α. Equilibrium depends on α and the trajectory to $\alpha = \beta = 0.9$ is the innermost. We note that the trajectories are very similar at first, but they differ over time.

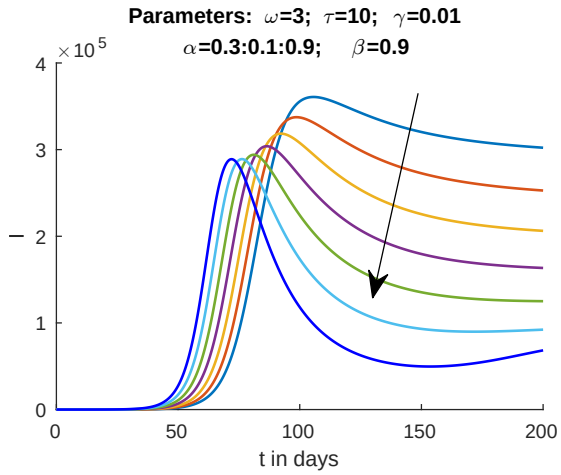

Figure 3: Effect of α in I.

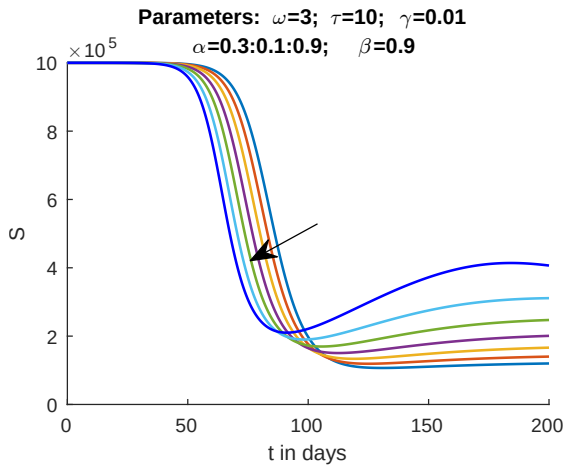

Figure 4: Effect of α in S.

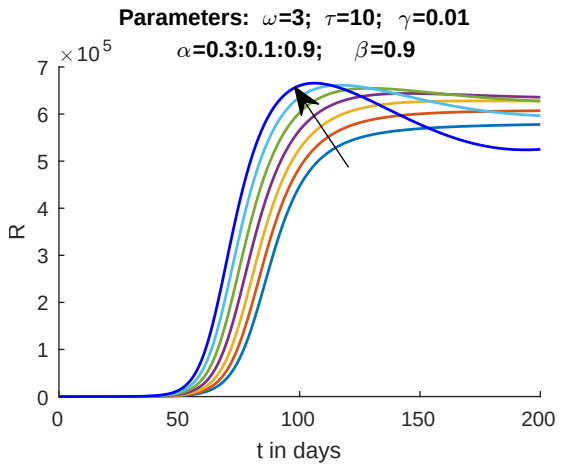

Figure 5: Effect of α in R.

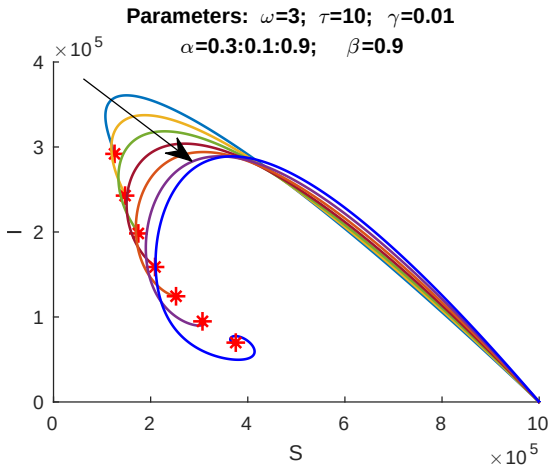

Figure 6: Effect of α - (S, I).

Now, we study the effect of the order β, which is related to intrinsic infectivity by Equation 32:
• (Effect of β in the ρ function) In Figure 7, we observe that increasing β makes the intrinsic infectivity smaller in the beginning, but larger over time. For $\beta = 1$, the function ρ is constant, that is, the disease does not change its infectivity over time, except for external factors, related to ω.

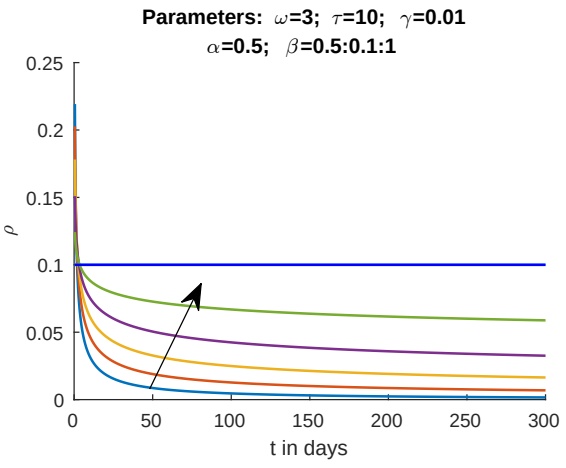

Figure 7: Effect of β in ρ.

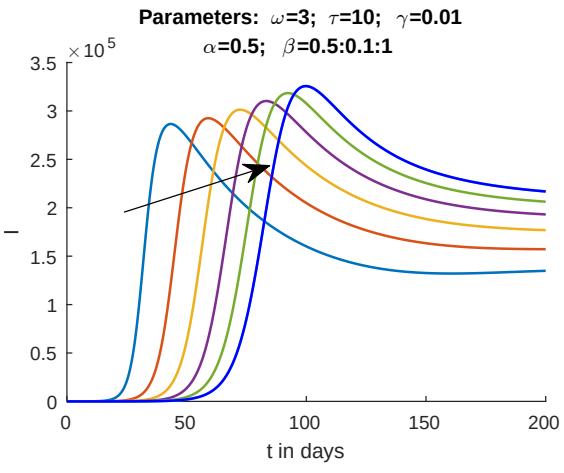

Figure 8: Effect of β in I.

• (Effect of β in the compartments) In Figures 8-10, we observe that, the higher the β, the longer the peak of infection takes to occur and is larger, although the profile of the infectious wave does not change much, as the β does not influence the ϕ permanence function. The amount of susceptibles decreases as β grows, but the wave is also delayed. Thus, β growing increases the epidemic, but at a later time, reflecting its effect in ρ.

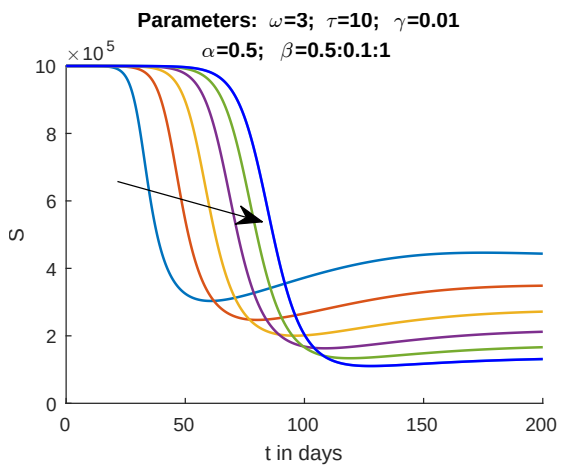

Figure 9: Effect of β in S.

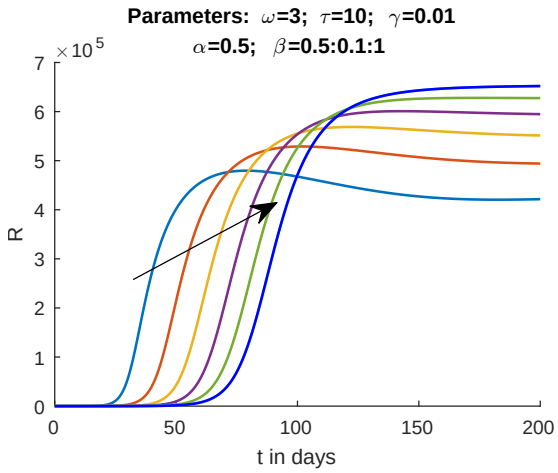

Figure 10: Effect of β in R.

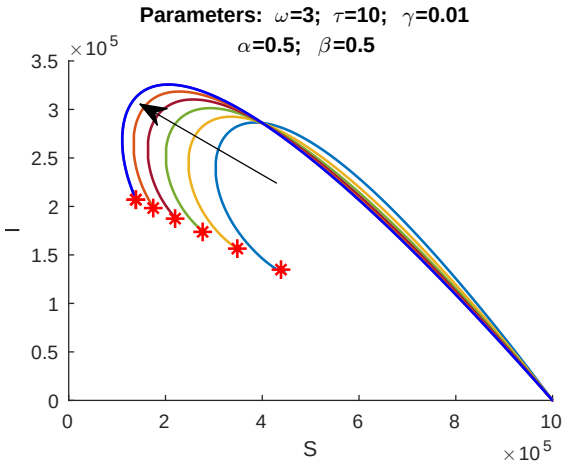

Figure 11: Effect of β $-(S, I)$.

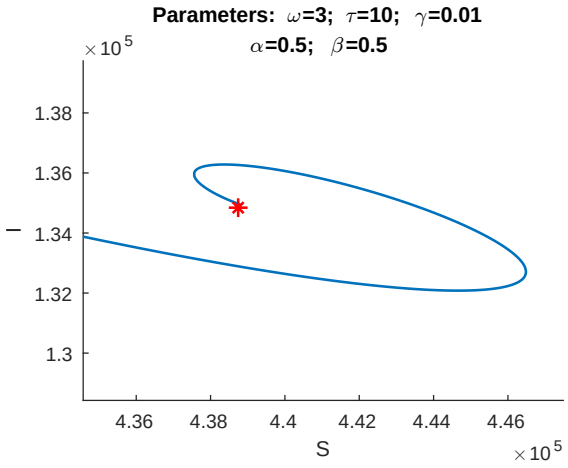

Figure 12: (S, I) (ZOOM).

• (Effect of β in the equilibrium) Figure 11 illustrates the equilibrium given in Eq. 24 for different orders β. Equilibrium depends on β and the trajectory to $\alpha = \beta = 0.9$ is the outermost one. We note that the trajectories are very similar at first, but they differ over time. In Figure 12, we observe the behavior of the trajectory close to the equilibrium point for $\beta = 0.5$.

Next, we analyze the effect of the parameter ω, the extrinsic infectivity given by Equation 6.

• (Effect of ω in the compartments) In Figures 13-15, we observe that the larger the ω, the greater and earlier the peak of infection occurs . The amount of susceptibles decreases faster as ω grows and the wave of removed occurs in a shorter amount of time. This was to be expected, as ω is concerned with extrinsic infectivity.

• (Effect of ω in the equilibrium) Figure 16 illustrates the equilibrium given in Eq. 24 for different choices of ω. Equilibrium depends on ω and the trajectory to $\omega = 4.5$ is the outermost one. As expected, the epidemic is greater if the extrinsic infectivity ω is greater.

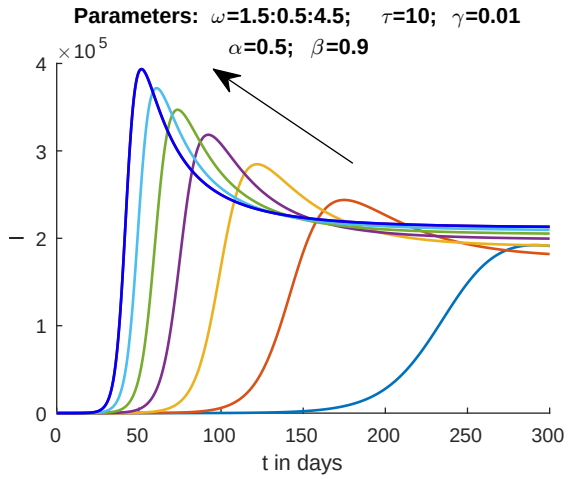

Figure 13: Effect of ω in I.

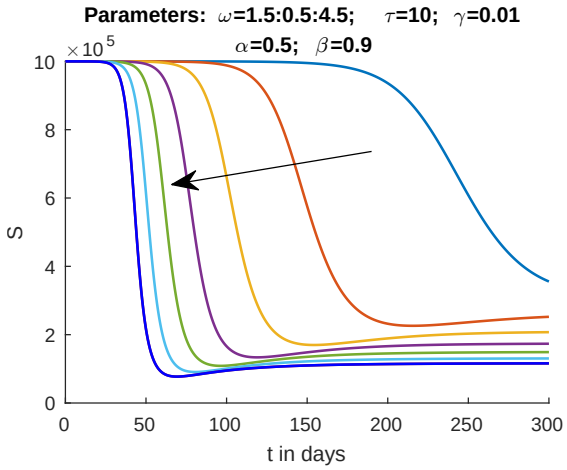

Figure 14: Effect of ω in S.

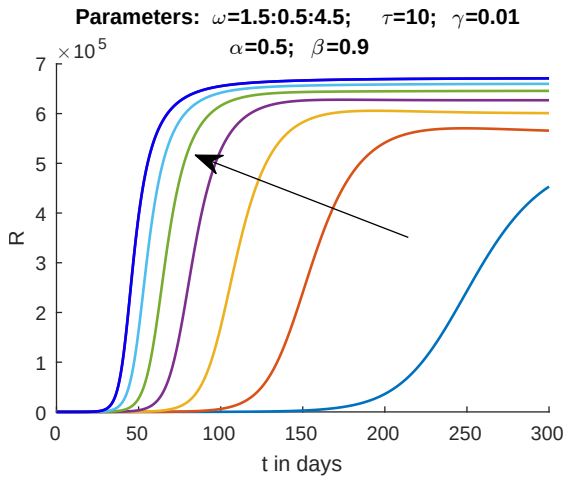

Figure 15: Effect of ω in R.

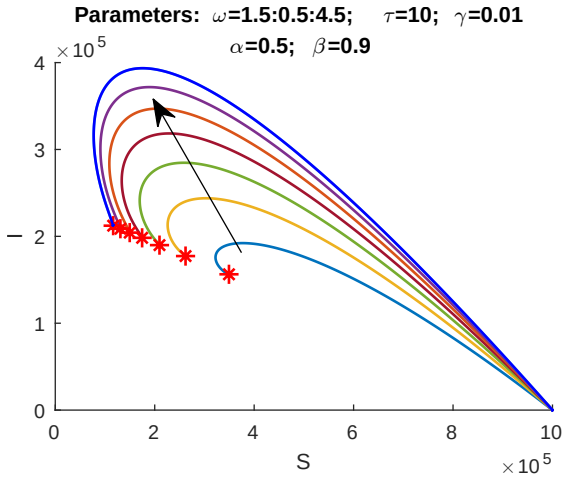

Figure 16: Effect of ω - (S, I).

Now, we analyze the effect of the parameter τ, the scale used in the Mittag-Leffler infectivity and removal functions. Remember that if $\alpha = \beta = 1$, τ is the average removal time.

• (Effect of τ in the functions ϕ and ρ) Figure 17 illustrates a slight increase in the permanence function independent of natural death as τ increases. On the other hand, Figure 18 indicates that, by increasing τ, we have a decrease in intrinsic infectivity. It is important to remember that ρ is constant for $\beta = 1$. Thus, if $\beta = 1$, the parameter τ does not influence the intrinsic infectivity.

• (Effect of τ in the compartments) In Figures 19-21, we observe that, as τ grows, the epidemic is translated forward, with only a slight decrease of the peak. Since τ is a time scale, this time shift behavior is expected. The slight decrease in the peak is due to the decrease in intrinsic infectivity, while the slight increase in the permanence function independent of natural death causes the peak to become somewhat thicker.

• (Effect of τ in the equilibrium) Figure 22 illustrates the equilibrium given in Eq. 24 for different choices of τ. Equilibrium depends on τ and the trajectory to $\tau = 7$ is the outermost one. We observe that the trajectories are very similar, since the mainly influence of the parameter τ is over time.

Finally, we analyze the effect of the parameter γ, the vital dynamics.

• (Effect of γ in the compartments) In Figures 23-25, we observe that increasing γ slows down the peak of the epidemic, even though it seems to delay its demise. This delay can be seen as an effect of the increased birth of new susceptible to infection.

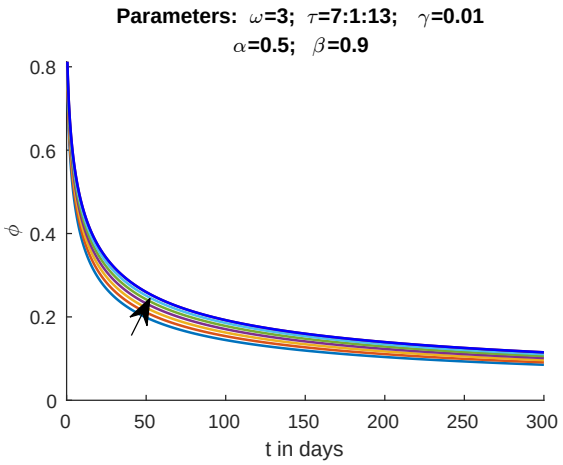

Figure 17: Effect of τ in ϕ.

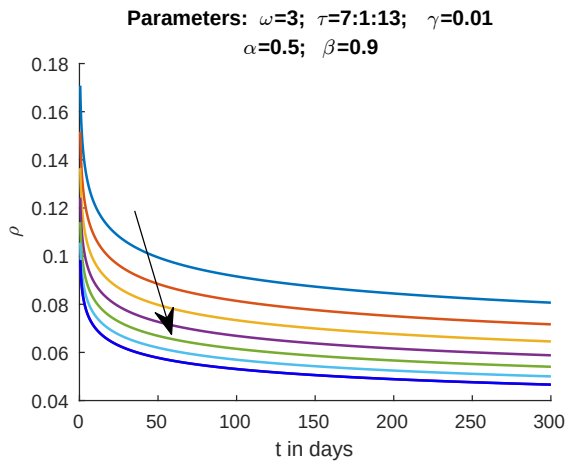

Figure 18: Effect of τ in ρ.

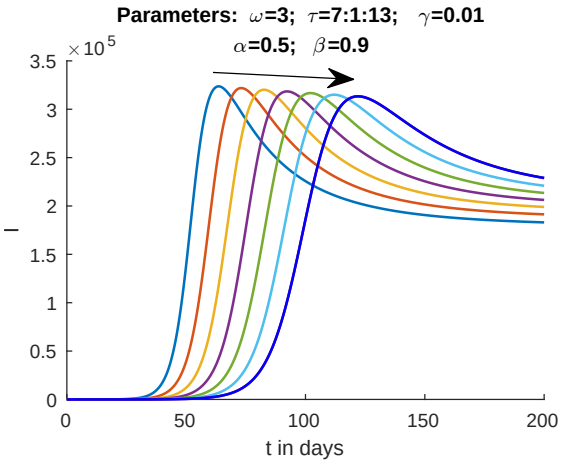

Figure 19: Effect of τ in I.

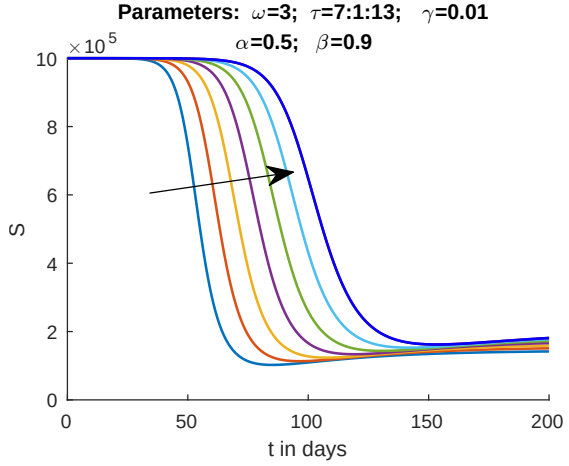

Figure 20: Effect of τ in S.

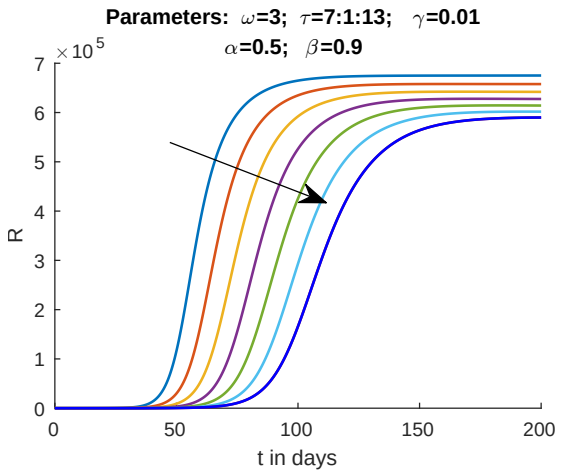

Figure 21: Effect of τ in R.

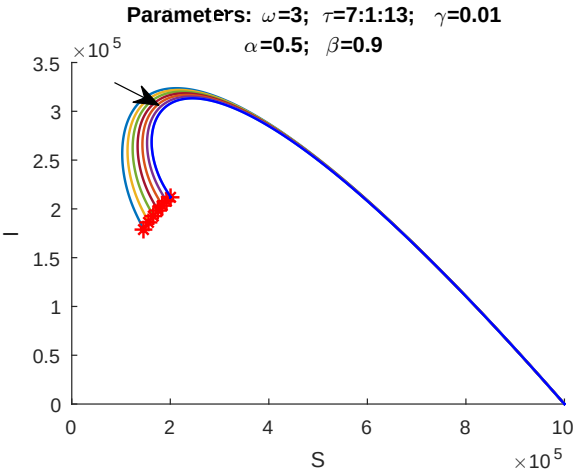

Figure 22: Effect of τ - (S, I).

• (Effect of γ in the equilibrium) Figure 26 illustrates the equilibrium given in Eq. 24 for different choices of γ. Equilibrium depends on γ and the trajectory to $\gamma = 0.004$ is the outermost one. We observe that the trajectories are very similar at first, but differ over time, with the epidemic being smaller when γ is larger. This is, we believe, due to the fact that high mortality induces a greater

decrease in the peak of infectious.

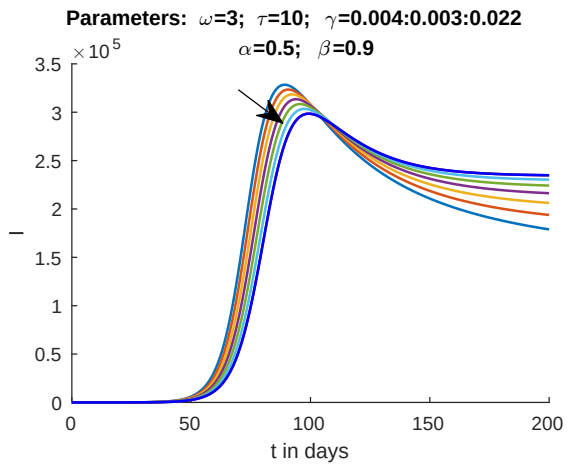

Figure 23: Effect of γ in I.

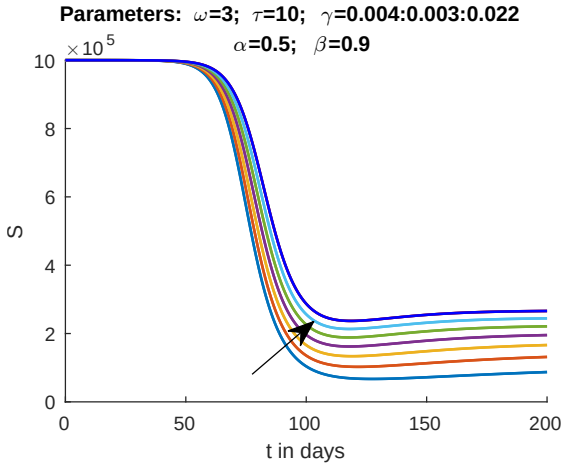

Figure 24: Effect of γ in S.

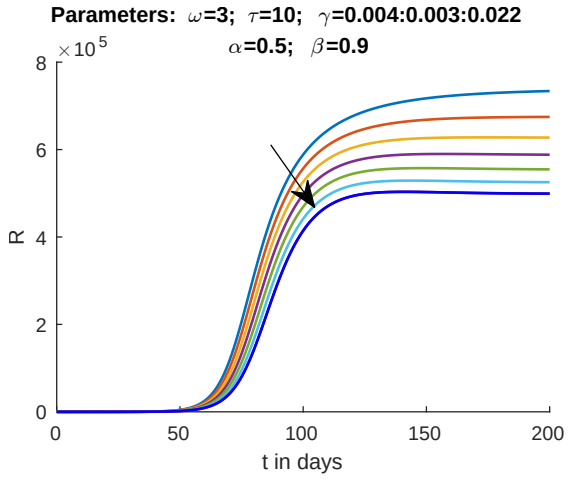

Figure 25: Effect of γ in R.

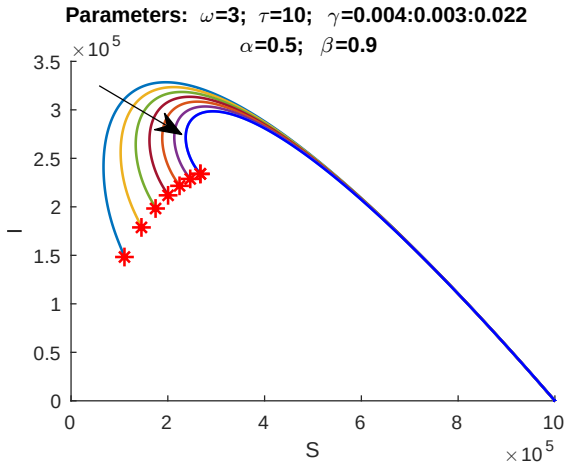

Figure 26: Effect of γ - (S, I).

In the next Subsection, we analyze some modifications of the simple model, through the introduction of the extrinsic infectivity $\omega(t)$ variable.

4.3 Variable extrinsic infectivity

Now, we consider ω with exponential decay, given by $\omega = \omega \cdot e^{-at}$. We consider $-at$ instead of $-t/a$, as we originally did in (MONTEIRO; MAZORCHE, 2021e), so that we can make the model with constant $\omega(t)$ be retrieved if $a = 0$. Next, we fix ω and analyze the effect of the a parameter.
• (Effect of a in the compartments) In Figures 27-29, we observe that increasing a reduces the peak of the epidemic and restores the susceptible compartment more quickly. This effect can be seen as a reflection of the monotonous decrease in extrinsic infectivity, for example, by prophylactic measures.
• (Effect of a in the equilibrium) Figure 30 illustrates the equilibrium given in Eq. 24 in red. We observe that the endemic equilibrium is reached only if the decay is null, that is, if ω is constant. Otherwise, since $\omega^* = \lim_{t\to\infty} \omega(t) = 0$, the equilibrium point is the disease-free one, $(N, 0, 0)$.

Now, we consider an oscillatory effect, defining $\omega = \omega \cos^2(b\pi t)$.

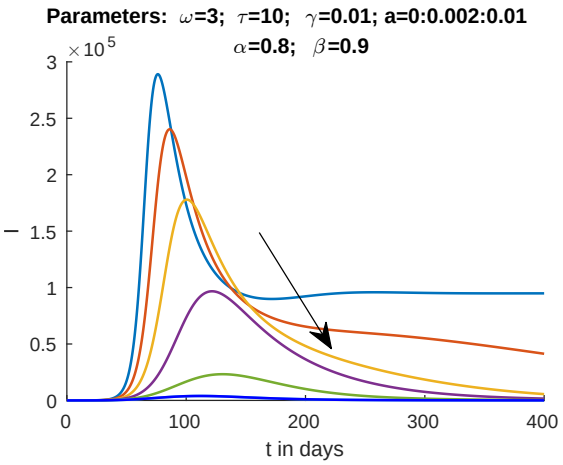

Figure 27: Effect of a in I.

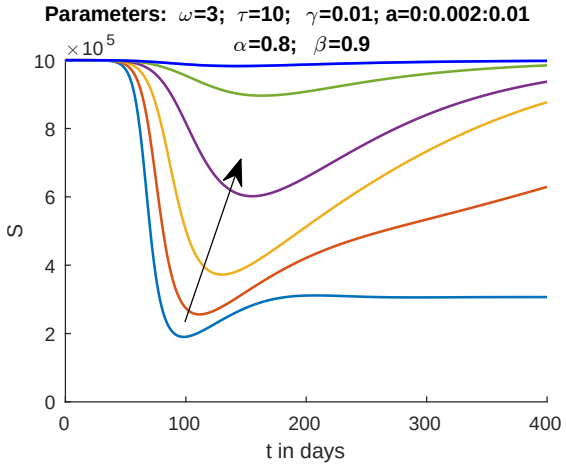

Figure 28: Effect of a in S.

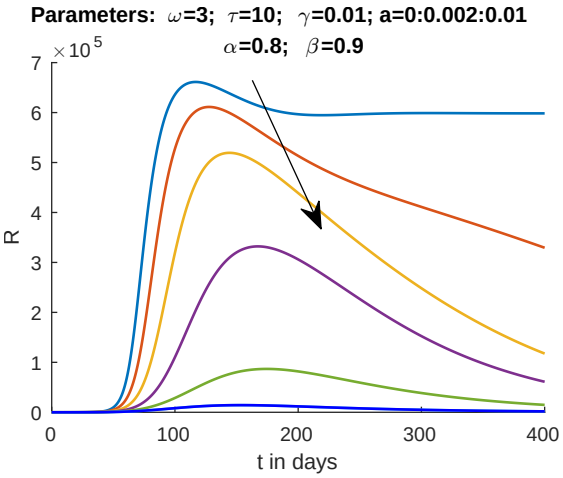

Figure 29: Effect of a in R.

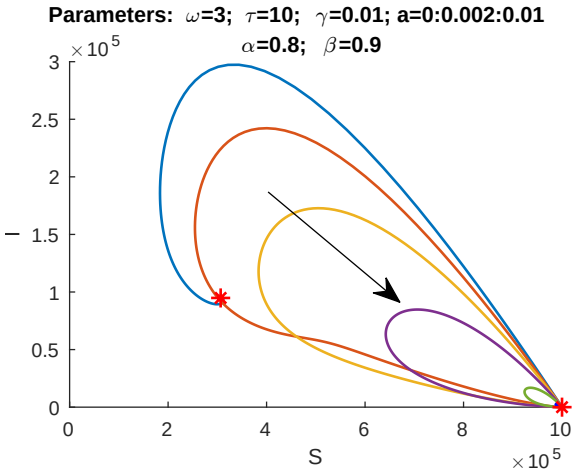

Figure 30: Effect of a - (S, I).

• (Effect of b in the compartments) In Figures 31-33, we observe that increasing b increases the number of waves of infection, for example, for alternating periods of relaxation and hardening of containment measures.

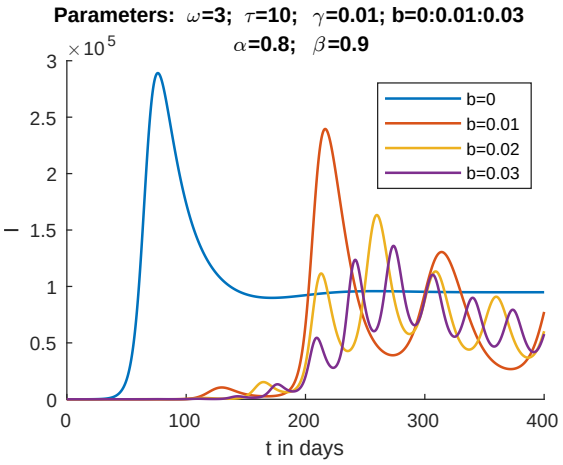

Figure 31: Effect of b in I.

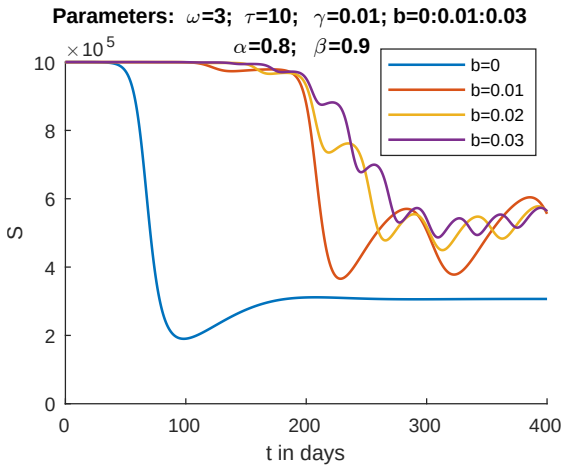

Figure 32: Effect of b in S.

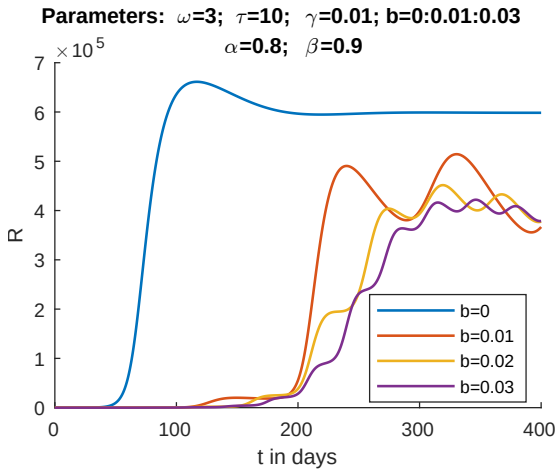

Figure 33: Effect of b in R.

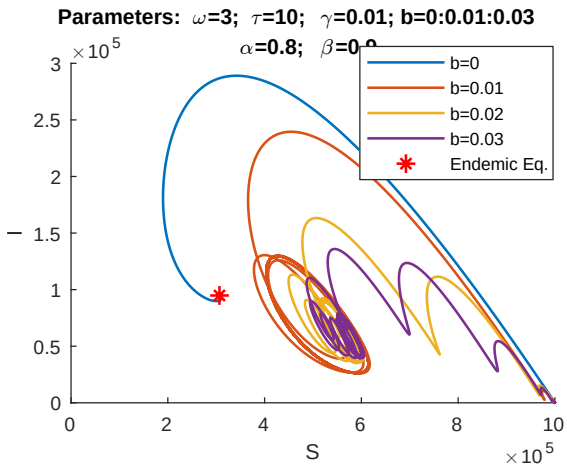

Figure 34: Effect of b - (S, I).

• (Effect of b in the equilibrium) Figure 34 illustrates the equilibrium given in Eq. 24, respected only if $b = 0$. In the presence of oscillation, the asymptotic equilibrium does not seem to exist. Finally, in Figures 35-36 we show particular examples of the combination of these two effects: $\omega = \omega \cdot e^{-at} \cos^2(b\pi t)$.

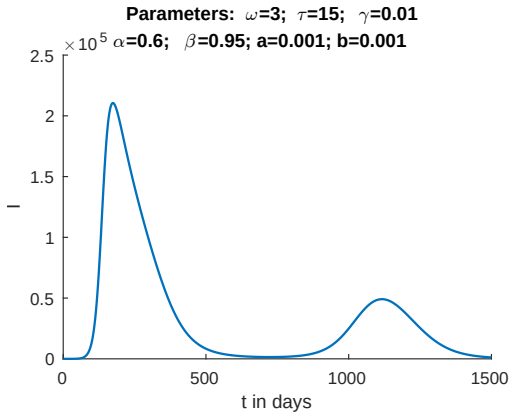

Figure 35: Oscillatory decay (1).

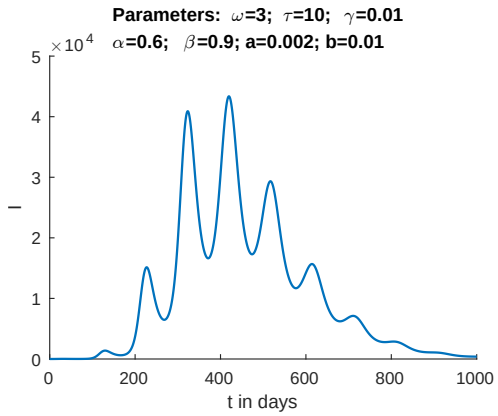

Figure 36: Oscillatory decay (2).

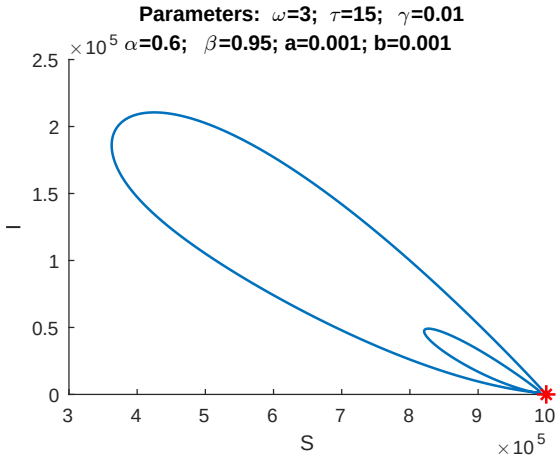

Figure 37: Osc. decay $-(S - I)$.

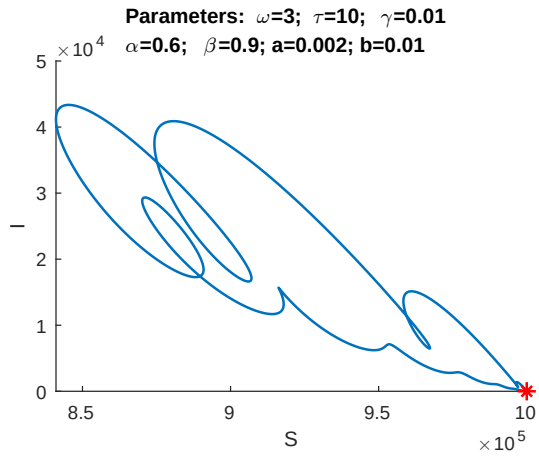

Figure 38: Osc. decay (2) $-(S - I)$.

The use of these parameters allows the phenomenon of waves and the extinction of the disease, through an oscillatory loss of extrinsic infectivity. This variation in infectivity can be seen, for example, as alternating periods of relaxation and tightening of containment measures, always pointing to a total dampening of the disease. In Figures 37-38, we display the respective trajectories. Since $\omega^* = 0$, the disease-free equilibrium is asymptotically stable.

5 Final considerations

As we see relevancy in applying the model to the data of COVID-19 and other diseases, the analysis can help in readjusting the parameters. It means, after a parametric readjustment, a new optimization can be more realistic.

However, the main focus here is that the numerical analysis step up the biological interpretation of the parameters. As an example, we cite the effect of the arbitrary orders α, related to the function of permanence in the infectious compartment, and β, related to the intrinsic infectivity. The smaller α, the heavier the tail of the permanence function in the infectious compartment, while, the larger α, the smaller the intrinsic infectivity function over time. Therefore, decreasing the α increases the asymmetry in the distribution of infectious, and increases the peak. By other hand, the higher the β, the longer the peak of infection takes to occur and is larger, although the profile of the infectious wave does not change much, as the β does not influence the permanence function ϕ. This kind of discussion validates and facilitates the meaningful use of the model, which is recent and little disseminated.

Acknowledgements. We appreciate the support of the Coordenação de Aperfeiçoamento de Pessoal de Nível Superior - Brasil (CAPES) - Financing Code 001.

References

ANGSTMANN, C. N.; HENRY, B. I.; MCGANN, A. V. A fractional-order infectivity and recovery sir model. **Fractal and Fractional**, Switzerland, v. 1, n. 1, p. 11, 2017.

KERMACK, W. O.; MCKENDRICK, A. G. Contributions to the mathematical theory of epidemics–i. 1927. **Bulletin of mathematical biology**, New York, v. 53, n. 1-2, p. 33–55, 1991.

MAZORCHE, S. R.; MONTEIRO, N. Z. Modelos epidemiológicos fracionários: o que se perde, o que se ganha, o que se transforma? **Proceeding Series of the Brazilian Society of Computational and Applied Mathematics**, Rio de Janeiro, v. 8, n. 1, 2021.

MONTEIRO, N. Z.; MAZORCHE, S. R. Analysis and application of a fractional sir model constructed with mittag-leffler distribution. *In*: IBERO-LATIN-AMERICAN CONGRESS ON COMPUTATIONAL METHODS IN ENGINEERING, 42, 2021, Rio de Janeiro. **Proceedings [...]**. Rio de Janeiro, 2021a.

MONTEIRO, N. Z.; MAZORCHE, S. R. Analysis results in an arbitrary order sir model constructed with mittag-leffler distribution. *In*: ENCONTRO NACIONAL DE ANÁLISE MATEMÁTICA E APLICAÇÕES, 2021, [Campina Grande]. **Proceedings** [...]. [S.l.]: Universidade Federal de Campina Grande e Universidade Estadual da Paraíba, 2021b.

MONTEIRO, N. Z.; MAZORCHE, S. R. Application of a fractional sir model built with mittag-leffler distribution. *In*: MATHEMATICAL CONGRESS OF THE AMERICAS, 2021, Buenos Aires. **Proceedings [...]**. Buenos Aires, 2021c.

MONTEIRO, N. Z.; MAZORCHE, S. R. Estudo de um modelo sir fracionário construído com distribuição de mittag-leffler. **Proceeding Series of the Brazilian Society of Computational and Applied Mathematics**, Rio de Janeiro, v. 8, n. 1, 2021d.

MONTEIRO, N. Z.; MAZORCHE, S. R. Fractional derivatives applied to epidemiology. **Trends in Computational and Applied Mathematics**, São Paulo, v. 22, p. 157–177, 2021e.

MONTEIRO, N. Z.; MAZORCHE, S. R. O cálculo fracionário e alguns de seus comportamentos incomuns. *In*: REUNIÃO MINEIRA DE MATEMÁTICA, 1, 2021, Juiz de Fora. **Proceedings** [...]. Juiz de Fora: Universidade Federal de Juiz de Fora, 2021f.

OLDHAM, K.; SPANIER, J. **The fractional calculus theory and applications of differentiation and integration to arbitrary order**. Amsterdam: Elsevier, 1974.

OLIVEIRA, E. C. **Solved exercises in fractional calculus**. New York: Springer, 2019.